Physicochemical and rheological properties of dietary fibres extracted from agri-food by products: comparison against methylcellulose

LWT - Food Science and Technology 232 (2025) 118408

Contents lists available at ScienceDirect

LWT

journal homepage: www.elsevier.com/locate/lwt

Physicochemical and rheological properties of dietary fibres extracted from agri-food by products: Comparison against methylcellulose

Whitney Vale-Hagan [a], Dimitris Charalampopoulos [b], Eoin Cunningham [c], Eric Whale [d], Anastasios Koidis [a,*]

[a] Institute of Global Food Security, School of Biological Sciences, Queen's University Belfast, Northern Ireland, Belfast, United Kingdom
[b] Department of Food and Nutritional Sciences, University of Reading, England, Reading, United Kingdom
[c] School of Mechanical and Aerospace Engineering, Queen's University Belfast, Northern Ireland, United Kingdom
[d] CelluComp Limited, Scotland, Dunfermline, United Kingdom

ARTICLE INFO

Keywords:
Dietary fibres
Agri-food byproducts
Extraction
Physicochemical properties
Rheological properties
Thermal stability

ABSTRACT

Fibres from different agri-food by products have varying physicochemical and functional properties that require further investigation in the context of sustainable food production to fundamentally understand the relationship between composition, structure and function. In this study, physicochemical and rheological properties of dietary fibres (DF) extracted from nine different sources namely apple pomace, wheat straw, hemp fibres, oat hulls, oat bran, pumpkin seeds, mushrooms compost, and coffee silverskin were compared to methylcellulose. The hydration, emulsifying, structural, and rheological properties were characterised. Hemp fibre (69.63 g/100g) and apple pomace (19.52 g/100g) had the relatively highest and lowest DF contents. Onion peels dietary fibre (OPDF) exhibited the highest water binding (0.94 g/g) and swelling capacities (13.85 mL/g). Methylcellulose (MC), acid-extracted apple pomace dietary fibre (AC-APDF) had the highest water holding capacities (12.74 g/g). MC was the only sample to exhibit excellent emulsification property with no serum layer observed. All DF samples and MC exhibited shear thinning behaviours with increasing shear rates. The spectral analysis showed that all DF samples contained characteristic peaks of polysaccharides. The findings correlate with results from PCA analysis and indicate the potential of DF from onion peels and apple pomace to act as a functional ingredient in the food industry.

1. Introduction

There has been a growing interest in the utilisation of agri-food by-products such as seeds, husks, pomace, hulls, stems, peels, pods, and pulp in recent years as raw materials for the extraction of dietary fibres (DF). Although there are several potential uses for these agri-food by-products they are often overlooked and discarded in the food industry. Such by-products possess inherent physicochemical and functional properties that render them useful resource materials for the food industry. Their use goes beyond being animal feed or as the primary material for biomass production. Recently, valorisation strategies have focused on extracting dietary fibres from a range of agri-food products including wheat, oats, citrus fruits, apples, carrots, and psyllium husk (Mateos-Aparicio, 2021). Findings suggest that DF have great potential of acting as thickening and stabilizing agents in food formulations. Moreover, multifunctional dietary fibres have been extensively studied for their beneficial effects on human health and their role in the food industry (Meng et al., 2021). These DF have been reported to have the potential to promote satiety and health, aid digestion, enhance food texture, stabilise emulsions, bind ingredients, and improve moisture retention (Chen et al., 2021; Zhang et al., 2023). The mentioned properties are mainly influenced by the physicochemical and functional properties of the DF.

A better understanding of the physicochemical properties enhances knowledge of DF behaviour in food matrices and their implications for food quality. These properties are often attributed to variation in the fibre chemical composition, geographical origin and extraction processes (Chen et al., 2021; Dong et al., 2023; Wang et al., 2017). It has been reported that the type of extraction method has different effects on the physicochemical properties of extracted DF (Lan et al., 2012;

* Corresponding author.
E-mail addresses: wvalehagan01@qub.ac.uk (W. Vale-Hagan), d.charalampopoulos@reading.ac.uk (D. Charalampopoulos), e.cunningham@qub.ac.uk (E. Cunningham), eric.whale@cellucomp.com (E. Whale), t.koidis@qub.ac.uk (A. Koidis).

https://doi.org/10.1016/j.lwt.2025.118408
Received 8 May 2025; Received in revised form 22 August 2025; Accepted 27 August 2025
Available online 28 August 2025

Moreover, Dong et al., 2023, found that the geographical origin of plant-based materials and agri-food by-products affects the physicochemical and functional properties of extracted DF. Additionally, the nature and type of raw materials have been shown to influence the functional, and structural properties of extracted DF (Gouw et al., 2017; Wu et al., 2024). To this end, recent studies have shown that DF from a range of origins such as fox millet, orange peels, de-oiled cumin, and bamboo shoots, etc have great potential to be used as functional ingredients in the food industry such as food binders and stabilisers (Gouw et al., 2017; Sánchez-Zapata et al., 2009; Zhu et al., 2018).

DF are versatile macromolecules with diverse functional properties. One of their key attributes is their ability to act as binding agents between water and other macromolecules such as proteins (Lu et al., 2019). The binding properties of DF is said to be influenced by their molecular structure, surface area, and overall charge density which enables them to interact with water, oil and other molecules through a combination of covalent, hydrogen bonding, electrovalent, polar and hydrophobic interactions (Luo et al., 2017; Zhang et al., 2023). DF work as binders by absorbing water, forming gels, and interacting with molecules or ions to form cohesive chains. The hydrophilic nature of DF, due to hydroxyl and carboxyl groups, enables water retention via hydrogen bonding, facilitating gel formation, which in turn creates a matrix that binds particles together (Feng et al., 2023). Also, most DF can increase viscosity which helps particles to suspend by reducing their movement and allowing them to stick together (Nasrollahzadeh et al., 2021, pp. 47–96). DF from pear pomace, bamboo shoot shell, de-oiled cumin were reported to have exhibited significant binding capacities to oil, water and glucose (Luo et al., 2018; Yan et al., 2019; Zhang et al., 2023). Understanding and optimising fibre binding properties enables innovative product development as well as sustainable practices through the valorisation of by-products.

Not all agri-food by-products have been explored as potential sources of DF. Currently, there is lack of comparative data evaluating DF extracted from widely accessible sources in UK and Ireland, such as apple pomace, oat hulls, oat bran, wheat straw, onion peels, pumpkin seeds, mushroom compost, hemp fibres, and coffee silver skin, alongside an industry standard food binder, methylcellulose (MC) using techno-functional, structural and rheological properties. (These sources are also common in other places in N. Europe and beyond). Due to the increasing interest in natural and sustainable ingredients, a thorough investigation of the DF's binding properties could provide useful insights into their application as alternatives to synthetic binders such as MC, contributing to the development of healthier and more environmentally friendly food products. MC production involves chemically modifying cellulose through an energy-intensive processes, often using chemicals like methyl chloride (Abolore et al., 2024). This process is considered unsustainable and may result in harmful waste generation and environmental emissions if not effectively managed. Therefore, to broaden the potential applications of DF in the food industry, it is essential to investigate their physicochemical and rheological properties.

Previous studies have demonstrated the potential of DF obtained from different sources having different physicochemical and functional properties (Dong et al., 2023; Kuan et al., 2011; Wu et al., 2024; Xie et al., 2017). Dong et al. (2023), demonstrated that DF from four different bamboo shoots, each from a different origin, showed variations in their water holding capacity (WHC) (10.00–13.05 g/g), oil holding capacity (OHC) (6.5–10.42 g/g) and swelling capacity (SC) (6.8–11.2 mL/g) as well as their microstructures. Wu et al. (2024) confirmed that DF from cereal brans from the same origin obtained using the same extraction methods had varying microstructures and intrinsic viscosities. On the other hand, Jacometti et al. (2015) reported that DF from different agri-product residues (rice hulls, oat hulls, banana pseudo stems and malt bagasse) presented low OHC (2.68 g of oil/g of DF) with DF from oat and rice hulls having no emulsification potential. Most existing research fails to provide detailed comparison of key parameters such as proximate, hydration, emulsification, rheological, and structural properties of DF from different agri-food by-products obtained via different extraction methods as compared to an industry standard food binder MC, as well as their exploitation as potential binding agent in the food industry.

The objective of this study was to extract and evaluate the binding efficiency of DF extracted from nine regionally available agri-food by products (apple pomace, oat hulls, oat bran, wheat straw, onion peels, pumpkin seeds, mushroom compost, hemp fibres, and coffee silver skin) benchmarking them against a commercially available food binder (MC) to assess their suitability as sustainable functional ingredients. By characterising the physicochemical and rheological properties of the extracted DF fractions, we seek to enhance our understanding on the functional potential of these by-products in food applications. The purpose of the study is to contribute to a broader understanding of how agri-food by-products can be utilised as functional ingredients in food formulations, thereby promoting sustainability and innovation in food research.

2. Materials and methods

2.1. Materials

The solvents, and chemicals, including the enzymes used in the study were of highest level of purity and of analytical grade. Specifically, all enzymes (a-amylase (activity; 0.34×10^{-4} to 1.00×10^{-3} kat) and Protease from *Bacillus licheniformis* (activity; $\geq 4.01 \times 10^{-8}$ kat) used were purchased from Sigma-Aldrich (Gillingham, UK). Food grade solvents (ethanol) were used for extraction. Food grade HCL and NaOH were obtained from Sigma-Aldrich. Agri-food by-products were obtained from local suppliers in the UK and Ireland. Mushrooms were obtained from Monaghan Mushrooms (Tyholland, Ireland), hemp fibre from a local farmer in Northen Ireland (Ian Marshall), *Triticum aestivum* (wheat) straw from Capper Trading Limited (Dungannon, Northern Ireland), apple pomace from Davisons Quality Foods- (Craigavon, Northern Ireland), onion peels from restaurants in Belfast, oat bran and oat hulls from White Oats (Tandragee, Northern Ireland), coffee silverskin from Lucid Coffee (Belfast, Northern Ireland), pumpkin seeds were collected from pumpkins sourced locally, and methylcellulose (commercial grade of high purity >0.99) from Sigma Aldrich (Gillingham, UK). Sunflower oil was purchased from a retailer.

2.2. DF extraction procedure

This study employed different methods of dietary fibre (DF) extraction based on the proximate composition and the nature of the materials. Fig. 1 below summarizes the different extraction methods used.

2.2.1. Extraction from wheat straw, hemp fibre and coffee silverskin

DF from wheat straw, hemp fibre and coffee silverskin was extracted following a protocol described previously (Yamazaki et al., 2005) with some modifications. About 100 g of ground samples were soaked in 1500 mL of 20 g/L NaOH in a Grant water bath for 2 h at 50 °C. The samples were transferred into 50 mL conical tubes and centrifuged at 4000×*g* for 15 min an Eppendorf centrifuge 5810 R (Eppendorf, Hamburg, Germany) with a swing bucket rotor (Rotor A-4-81). The supernatant was discarded, and precipitates were washed with 20 g/L NaOH solution and centrifuged at 4000×*g* for 15 min using the same centrifuge, rotor (Rotor A-4-81) and conical tubes as mentioned above. The insoluble fraction precipitates were collected and soaked in 1000 mL of 36.46 g/L HCl solution for 2 h at 50 °C. The mixture was centrifuged at 4000×*g* for 15 min using the same centrifuge, rotor (Rotor A-4-81) and conical tubes as mentioned above and washed with 18.23 g/L HCl solution. Precipitates were collected and washed with distilled water and insoluble DF were collected, freeze dried using the Lablyo Plus freeze dryer (Frozen in Time Limited, York, England, United Kingdome) for 48 h, milled using a high-speed multifunction grinder for

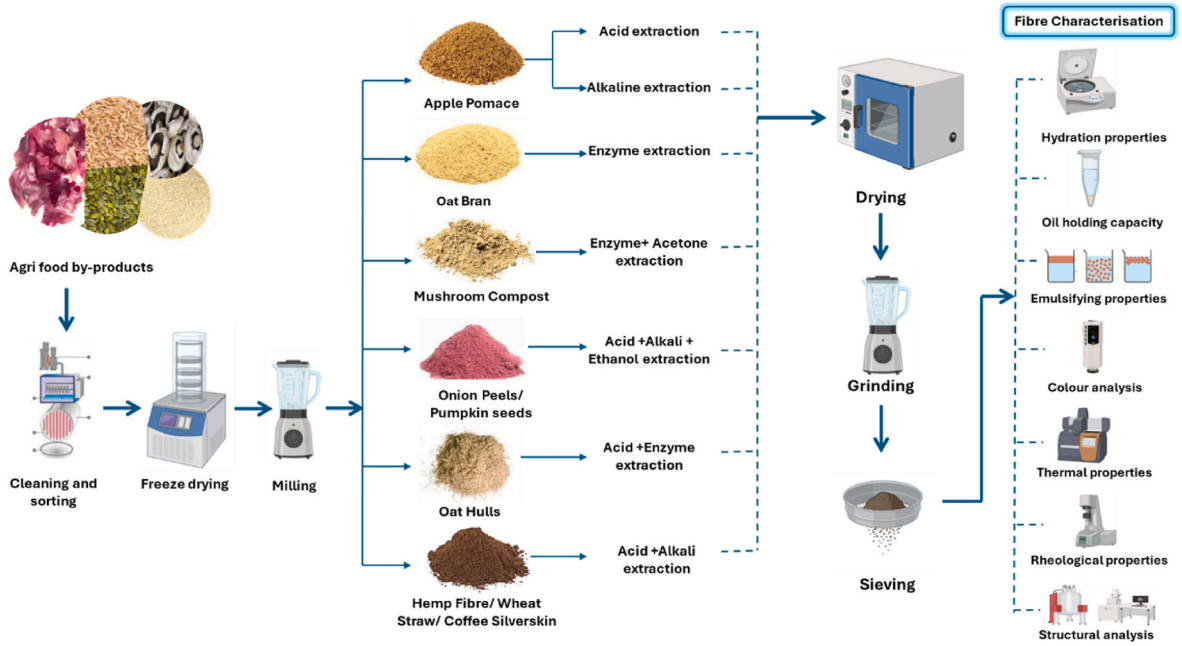

Fig. 1. Workflow for DF extraction and characterisation: methodology overview. Created in BioRender. Vale-hagan, W. (2025) https://BioRender.com/nlqddlc.

3 min (1 min rest for every minute of grinding) (CGOLDWALL, Dorchester Centre, Massachusetts, USA) and passed through a 35 μm sieve. The DF were kept at 4 °C until needed.

2.2.2. Extraction from oat hulls

DF was extracted from oat hulls according to a protocol described by (Wen et al., 2017) with some modifications. About 100 g milled oat hulls were soaked in 1000 mL of deionized water for 90 min at 50 °C in a water bath. The mixture was then transferred into 50 mL conical tubes and centrifuged at 4000×*g* for 15 min with an Eppendorf centrifuge 5810 R (Eppendorf- Germany) with a swing bucket rotor (Rotor A-4-81). The resulting residue were soaked in 100 0 mL of 30.00 g/L NaOH for 120 min at 50 °C. The pH of the mixture was adjusted using 18.23 g/L HCl and incubated at 100 °C for 15 min. Exactly 1 g (1g/100g of sample) of heat resistant ɑ-amylase (activity; 34×10^{-4} to 1.00×10^{-3} kat) was added to the slurry and kept at 95 °C for 40 min. The slurry was centrifuged at 4000×*g* for 5 min with an Eppendorf centrifuge 5810 R (Eppendorf- Germany) with a swing bucket rotor (Rotor A-4-81) in 50 mL conical tubes and washed with distilled water. The precipitates were freeze dried, milled and passed through a 35 μm sieve. The fibres were kept at 4 °C until needed.

2.2.3. Extraction from onion peels and pumpkin seeds

DF from onion peels and pumpkin seeds were extracted following a protocol described by (Meng et al., 2021) with some modifications. Samples were freeze dried, milled and refluxed with 700 mL/L ethanol to get rid of low molecular weight compounds. About 100 g of refluxed powders were soaked in 1500 mL of deionized water and the pH was adjusted to 2.0 with 182.30 g/L HCl. The mixture was incubated at 90 °C for 90 min and centrifuged at 4000×*g* with Eppendorf centrifuge 5810 R (Eppendorf, Hambourg, Germany), with a swing bucket rotor (Rotor A-4-81) in 50 mL conical tubes. The supernatant was discarded, and precipitates were incubated at 75 °C using 30.00 g/L NaOH for 2 h. After, the mixture was centrifuged at 4000×*g* using Eppendorf centrifuge 5810 R (Eppendorf, Hamburg, Germany), with a swing bucket rotor (Rotor A-4-81) in 50 mL conical tubes and residues were precipitated in 800 mL/L ethanol at 4 °C overnight. The mixture was centrifuged with the same parameters above, and the remaining residues were washed with deionized water. Samples were freeze dried using the Lablyo Plus freeze dryer (Frozen in Time Limited, York, England, United Kingdome) for 48 h, milled using a high-speed multifunction grinder for 3 min (1 min rest for every minute of grinding) (CGOLDWALL, Dorchester Centre, Massachusetts, USA), and passed through a 35 μm sieve. DF were kept at 4 °C until needed.

2.2.4. Extraction from oat bran

DF from oat bran was extracted following a previously described protocol by (Guo et al., 2021) with some modification. About 20g of milled oat bran samples were suspended in 0.2L deionized. The pH of the slurry was adjusted to 6.0 using 18.23 g/L HCl and 0.32 g of heat resistant ɑ-amylase (activity; 34×10^{-4} to 1.00×10^{-3} kat) was added and incubated at 60 °C for 40 min in an agitating water bath. The temperature was allowed to drop to 40 °C and 0.16 g of protease from *Bacillus licheniformis* (activity; $\geq 4.01 \times 10^{-8}$ kat) was added. The slurry was left to digest for 2 h at 40 °C and centrifuged at 4000×*g* for 15 min with an Eppendorf centrifuge 5810 R (Eppendorf- Germany), with a swing bucket rotor (Rotor A-4-81) in 50 mL conical tubes. After, the supernatant was discarded and residue were freeze dried, milled, and passed through a 35 μm sieve. Fibres were kept at 4 °C until needed.

2.2.5. Extraction from apple pomace

Both acid and alkali methods were used in extracting fibres from apple pomace following the protocol described by (Fidriyanto et al., 2023). For acid extraction, 100 g of freeze dried and milled apple pomace was dispersed in 2000 mL of water and pH was adjusted to 2.0 using 182.30 g/L HCl. After, the mixture was agitated for 4 h in a shaking water bath at 80 °C. For alkaline extraction, 100g of freeze dried and milled apple pomace was mixed with 2000 mL of 2.00 g/L NaOH and pH was adjusted to 7 using a 182.30 g/L HCl solution. The mixture was stirred on a hot plate at 45 °C for 4 h. After incubation, both acid and alkali apple pomace slurries were centrifuged separately at 4000×*g* for 15 min with an Eppendorf centrifuge 5810 R (Eppendorf- Germany), with a swing bucket rotor (Rotor A-4-81) in 50 mL conical tubes. The supernatants were discarded, and precipitates were washed with deionized water twice. The residues were freeze dried, milled, and passed through a 35 μm sieve. Fibres were kept at 4 °C until needed. and dried using the freeze drier.

2.2.6. Extraction from mushroom compost

DF were extracted from *Agaricus bisporus* mushrooms according to a previously described protocol by (Jia et al., 2020) with some modifications. About 50 g of freeze dried and milled *Agaricus bisporu* mushrooms were weighed and dispersed in 1000 mL of distilled water. The pH of the mixture was adjusted to 7.0 and the mixture was hydrolysed with 0.75 g heat-resistant ɑ-amylase (activity; 34×10^{-4} to 1.00×10^{-3} kat) (1.5 g of enzymes/100 g of sample). at 60 °C for 2 h. After the temperature was adjusted to 40 °C and mixture was hydrolysed with 0.6g protease from Bacillus licheniformis (activity; $\geq 4.01 \times 10^{-8}$ kat) (1.2 g of enzymes/100 g of sample). After, the mixture was centrifuged at 4000×*g* using Eppendorf centrifuge 5810 R (Eppendorf, Hamburg, Germany), with a swing bucket rotor (Rotor A-4-81) in 50 mL conical tubes. The supernatant was discarded, and the residue were precipitated with four volumes of 900 mL/L ethanol for 1 h at 4 °C. After precipitates were collected and washed three times with acetone. The residues were freeze dried, milled, and passed through a 35 μm sieve. Fibres were kept at 4 °C until needed. and dried using the freeze drier.

2.3. Proximate compositional analysis of extracted DF

The moisture contents were determined using the oven drying method per AOAC 925.10, crude protein were determined using Dumas method per AOAC 992.23, crude fibre was determined by a gravimetric method per AOAC 962.09, ash contents were determined using dry ashing method by AOAC 923.03 and fat contents using the Soxhlet extraction method as described by AOAC 920.39. The carbohydrates content was calculated by difference: 100g - (moisture + ash + protein + fat + fibre) based on the Association of Analytical Chemists (AOAC) protocol (AOAC, 2016). The fibre composition analysis including extractives, cellulose, hemicellulose and lignin contents was determined using Ankom Analyser's fibre analysis protocol.

2.4. Water holding capacity, swelling capacity and water binding capacity

The water holding capacity (WHC) and water binding capacity (WBC) of the various DF were determined according to a previously described protocol (Qiu et al., 2017). WHC and WBC were calculated using the equation:

$$WHC = \frac{mw - m}{m} \quad (1)$$

$$WBC = \frac{mw - mb}{mw} \quad (2)$$

Where: m_w is the weight of the samples following water absorption (g), m is the weight of the samples before water absorption, and m_b is the weights of the samples after drying. Both WHC and WBC measurement for each sample was done in triplicate.

The swelling capacity (SC) of the DF were determined following a previously described protocol (Qiu et al., 2017). SC was expressed as the volume change after water swelling:

$$SC = \frac{V2 - V1}{m0} \quad (3)$$

Where: V_2 is the volume of the samples after water absorption (mL), V_1 is the volume of the fibre samples before water absorption (mL) and m_o is the weights of the samples (g). The SC measurement for each sample was done in triplicate.

2.5. Oil holding capacity

The oil holding capacity (OHC) of the DF was determined according to a previously described protocol (Qiu et al., 2017). OHC was calculated using the equation:

$$OHC = \frac{mo - m}{m} \quad (4)$$

Where: m_o is the weight of the samples following oil absorption (g) and m is the weight of the samples before oil absorption. The OHC measurement for each sample was done in triplicate.

2.6. Particle size analysis

The particle size of the dietary fibres was measured using a particle size laser analyser (Mastersizer 3000, Malvern Panalytical Co., Ltd., UK). The refractive indices of dispersants were (1.33) and of samples were 1.36 for AL-APDF and AC-APDF; 1.53 for WSDF, OHDF, HFDF, and PSDF; 1.6 for CSDF and MCDF; 1.47 for OBDF and 1.4 for OPDF, respectively. Each sample was dispersed in circulating water and treated with ultrasonic vibration until it met the laser signal conditions. The particle size was calculated and expressed in terms of the Dv 10 (μm), Dv 50 (μm), Dv 90 (μm) and span values.

$$Span = \frac{D90 - D10}{D50} \quad (5)$$

Where: D10 is the particle diameter at the 0.10 vol fraction of the distribution, D50 is the particle diameter at the 0.50 vol fraction of the distribution and D90 is the particle diameter at the 0.90 vol fraction of the distribution.

2.7. Emulsifying activity and stability

Emulsifying activity (EA) and stability (ES) were determined following a previously described protocol (Xie et al., 2017) with some modifications. The emulsion was homogenised at 13500 rpm for 5 min (30 s rest for every minute of homogenization) and centrifuged at 4500 rpm for 15 min with an Eppendorf centrifuge 5810 R (Eppendorf- Germany) rotor (Rotor A-4-81) in a 50 mL conical tubes. Emulsifying activity was calculated as: EA was calculated as:

$$EA\left(\frac{mL}{100mL}\right) = \frac{He}{Ht} X\,100 \quad (6)$$

Where: H_t is the total height of the emulsion and H_e is the height the emulsified layer, respectively.

ES was calculated as follows:

$$ES\left(\frac{mL}{100mL}\right) = \left(\frac{V1}{V}\right) X\,100 \quad (7)$$

Where: V and V1 are the volumes of the emulsified layer before heating and the layer after heating, respectively. For each experiment, group differences were analysed independently via one-way ANOVA with post-hoc corrections (Tukey's test). Data variability is presented as error bars of the Standard error of mean (SEM), calculated as standard deviation divided by the square root of sample size ($SD/\sqrt{n}$).

2.8. Rheological analysis

The rheological properties of the DF samples (5g of solids/100 mL) were tested using an AR-G2 Rheometer, (TA Instruments, Elstree, United Kingdom) according to a previously described protocol (Eren et al., 2015) with some modifications. A stainless-steel parallel plate (40 mm) was used to run an apparent viscosity and temperature sweep tests. For flow behaviour, a steady shear experiment was performed at an increasing shear rate from 0.01 to 10/s with a gap of 2000 μm. For oscillatory tests, a strain sweep test was carried out with a strain range from 0.0001 to 10 to establish the linear viscoelastic region (LVR) of the samples. A temperature sweep test was performed at a strain value of 0.001 within the LVR, with an increasing temperature from 20 to 85 °C,

at a frequency of 1Hz and a ramp rate of 5 °C.

2.9. Structural analysis

2.9.1. FTIR spectroscopy

The FTIR spectra of DF samples were obtained by using a Nicolet iS50 FT-IR Infrared spectrometer (Thermo Fisher Scientific Co. Ltd., Waltham, Massachusetts, USA). The range of wavelengths was 4000-400 cm^{-1}, resolution of 4 cm^{-1}; 64 scans were conducted. A graph of relative transmittance was plotted against wavelength (Liu et al., 2020).

2.9.2. Scanning electron microscopy (SEM)

The morphology of the DF samples was observed and photographed with a scanning electron microscope (TESCAN LYRA3, Brno, Czech Republic) at 1000 × . A copper plate was attached to a sample stage and the samples were placed on the copper stage and spattered with gold. The surface morphology of the samples was observed at a working beam of 5 kV and a speed scan of 3 with an emission gun as the source of electron field.

2.10. Statistical analysis

All experiments were performed in triplicate for each sample and results were expressed as means ± standard deviations (SD). All charts were created using either Excel or GraphPad prism 9. Using SPSS version 26 software, one-way ANOVA and Tukey's test were performed to compare means of different groups. A P value < 0.05 demonstrated significant difference. All values were tested for normality using SPSS version 26. Using Origin Pro, Principal Component Analysis (PCA) analyses were performed and plotted to further explore the relationships and patterns within the dataset.

3. Results and discussion

3.1. Fibre composition analysis

Table 1 shows the proximate analysis of the different DF samples in terms of their moisture, fat, crude fibre, protein, ash and carbohydrate contents.

The proximate composition plays a crucial role in determining the functional properties and potential applications of the fibres in various industries, such as food, nutraceuticals or material science. The moisture contents of the samples ranged from 2.81 **g/100g** for MC to 8.04 **g/100g** for coffee silverskin dietary fibre (CSDF), with most of the samples being in the range of 4–8 **g/100g**. The results obtained were similar to moisture contents of other DF samples (6.95–9.08 **g/100g**) (López-Marcos et al., 2015). The moisture content plays an important role in applications such as water-binding and water retention. Based on the results obtained, samples with higher moisture content had lower water binding capacities and vice versa. The crude fibre content of the DF samples varied greatly ranging from 3.24 **g/100g** oat bran dietary fibre (OBDF) to 96.41 **g/100g** (MC). MC, HFDF, and wheat straw dietary fibre (WSDF) had the highest crude fibre content indicating that they are predominantly fibrous materials. MC was a commercial sample with a purity content of >90 parts per 100. OBDF had relatively lower fibre content below 10 **g/100g**. All other samples had fibre contents of >30 **g/100g**. The fat content of the fibres ranged from 0.05 **g/100g** (MC) to 28.61 **g/100g** pumpkin seeds dietary fibre (PSDF) with most samples having a fat content below 10 **g/100g**. PSDF (28.61 **g/100g**) had a notably high fat content compared to the other samples, making it suitable for applications where a higher lipid content is desirable, such as in functional foods or dietary supplements that require a source of healthy fats. However, for the purpose of the application of fibres as hydrocolloids, a higher fat content may interfere with the gelation, binding and thickening ability as this reduces the number of available sites for water interaction. Onion peels dietary fibre (OPDF) (0.16 **g/100g**), and MC (0.05 **g/100g**) had very low-fat contents which makes them suitable for the application as hydrocolloids in food. Similarly, DF samples from some agri-products presented a higher variation in fat content (0.48–20.96 **g/100g**) with pomegranate seeds DF having a fat content of 20.9 **g/100g**, tiger nut (9.85 **g/100g**) and lemon albedo (7.22 **g/100g**) fibres had moderate levels, while grapefruit dietary fibre (0.48 **g/100g**) was lowest (López-Marcos et al., 2015). The total mineral content of the DF samples, as determined by ashing, ranged from 0.31 **g/100g** for MC to 1.46 **g/100g** for hemp fibre dietary fibre (HFDF). The variations in the ash contents could be attributed to the nature and source of materials used. The protein content of the DF samples varied significantly with mushroom compost dietary fibre (MCDF) showing the highest value (33.46 **g/100g**) and MC the lowest (0.06 **g/100g**). The protein content of MC was below the detectable limits. OPDF (0.77 **g/100g**), HFDF (0.77 **g/100g**), WSDF (0.78 **g/100g**), and oat hulls dietary fibre (OHDF) (0.58 **g/100g**) had very low protein contents of less than 1 **g/100g**. However, MCDF and OBDF had comparatively higher protein contents. Carbohydrate content is usually measured by difference in proximate analysis, which includes all organic components not quantified as protein, fat, moisture, ash, or fibre. Sugars, starches, and non-fibre polysaccharides often constitute most of the available carbohydrate. The carbohydrates content of the DF samples ranged from 0.23 **g/100g** (PSDF) to 64.96 **g/100g** (OBDF). The variation in the chemical composition is an indication of the different sources and processing techniques used, highlighting the importance of tailoring these factors to achieve specific physicochemical and functional properties.

Fig. 2 presents the fibre compositional analysis for the various DF samples based on their percentages of extractives, hemicellulose, cellulose and lignin. Each sample presents a unique profile, reflecting the variability in the composition of the different DF samples. The

Table 1
Proximate composition of extracted dietary fibre samples from various agri-food by-products sources.

Sample code	Moisture (g/100g)	Fat (g/100g)	Ash (g/100g)	Crude fibre (g/100g)	Protein (g/100g)	CHO (g/100g)
OBDF	7.67 ± 0.11^{a}	8.75 ± 1.84^{a}	0.49 ± 0.05^{a}	3.24 ± 0.33^{a}	14.89 ± 0.04^{a}	64.96 ± 2.20^{a}
HFDF	3.83 ± 0.13^{b}	1.01 ± 0.38^{d}	1.46 ± 0.21^{b}	81.57 ± 2.12^{b}	0.77 ± 0.02^{bc}	11.36 ± 2.75^{b}
AC-APDF	4.28 ± 0.25^{bc}	7.55 ± 0.00^{ab}	1.21 ± 0.21^{c}	44.28 ± 2.46^{c}	5.48 ± 0.15^{d}	37.20 ± 2.91^{cd}
AL-APDF	4.12 ± 0.31^{b}	4.82 ± 1.10^{bc}	0.76 ± 0.00^{d}	34.92 ± 0.96^{d}	4.83 ± 0.01^{e}	50.55 ± 0.30^{f}
OHDF	7.40 ± 0.04^{a}	0.22 ± 0.31^{d}	1.05 ± 0.21^{e}	54.04 ± 0.56^{e}	0.58 ± 0.01^{b}	36.71 ± 0.31^{ce}
WSDF	5.62 ± 0.08^{d}	0.67 ± 0.13^{d}	1.21 ± 0.22^{e}	72.70 ± 0.70^{f}	0.78 ± 0.01^{c}	19.02 ± 0.99^{b}
PSDF	5.27 ± 0.05^{cd}	28.61 ± 0.95^{e}	0.89 ± 0.27^{f}	53.56 ± 0.16^{e}	11.44 ± 0.05^{f}	0.23 ± 0.02^{g}
CSDF	8.04 ± 0.31^{a}	2.21 ± 0.04^{cd}	0.34 ± 0.16^{g}	52.95 ± 0.39^{e}	13.63 ± 0.01^{g}	22.83 ± 0.56^{b}
MCDF	6.61 ± 0.66^{d}	1.80 ± 0.12^{d}	1.05 ± 0.21^{h}	51.10 ± 2.03^{e}	33.46 ± 0.00^{h}	5.98 ± 0.62^{h}
OPDF	7.71 ± 0.13^{a}	0.16 ± 0.04^{d}	0.88 ± 0.11^{g}	53.82 ± 0.68^{e}	$0.77 \pm 0.03b^{c}$	36.67 ± 0.28^{e}
MC	2.81 ± 0.20^{b}	0.05 ± 0.00^{d}	0.31 ± 0.03^{c}	96.41 ± 2.10^{g}	0.06 ± 0.01^{i}	0.36 ± 0.02^{e}

NB: all data are means and S.D. of triplicate measurements; different letters denote significant difference in the column at $P < 0.05$. OHDF: oat hulls dietary fibre, WSDF: wheat straw dietary fibre, AL-APDF: alkaline extracted apple pomace dietary fibre, AC-APDF: acid extracted apple pomace fibre, OPDF: onion peels dietary fibre, MCDF: mushroom compost dietary fibre, HFDF: hemp fibre dietary fibre, CSDF: coffee silverskin dietary fibre, OBDF: oat bran dietary fibre, PSDF: pumpkin seed dietary fibre, MC: methylcellulose.

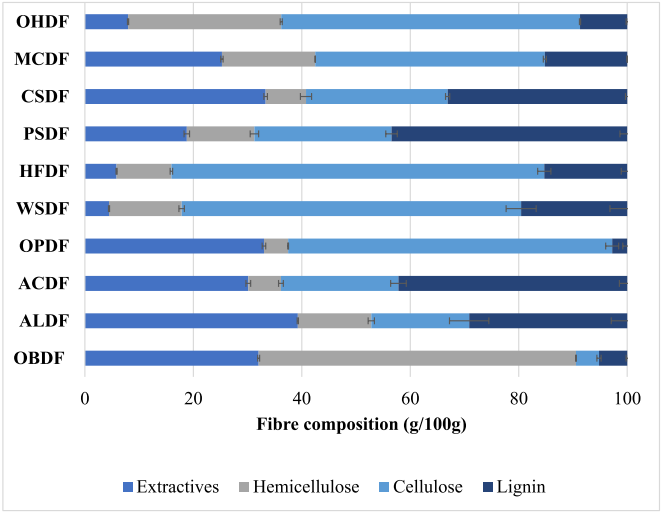

Fig. 2. Fibre compositional analysis of the dietary fibre samples obtained from various agri-food by-products sources.
Notes: OHDF: oat hulls dietary fibre, WSDF: wheat straw dietary fibre, AL-APDF: alkaline extracted apple pomace dietary fibre, AC-APDF: acid extracted apple pomace fibre, OPDF: onion peels dietary fibre, MCDF: mushroom compost dietary fibre, HFDF: hemp fibre dietary fibre, CSDF: coffee silverskin dietary fibre, OBDF: oat bran dietary fibre, PSDF: pumpkin seed dietary fibre, MC: methylcellulose.

extractives content represents the pectin, sugars, lipid and protein contents in the DF samples. The DF samples exhibit a wide range of extractives from as low as 4.45 **g/100g** (WSDF) to as high as 39.26 **g/100g** (AL-APDF). A higher extractive content in OBDF and AL-APDF may indicate the presence of higher non-fibrous components such as pectin, protein and fats. As illustrated in Table 1, OBDF had the lowest crude fibre content but relatively higher carbohydrate and protein components. The hemicellulose content of the samples ranged from 4.46 **g/100g** (OPDF) to 58.52 **g/100g** (OBDF). Cellulose was the most dominant component in many of the samples with values ranging from 4.24 **g/100g** (OBDF) to 68.76 **g/100g** (HFDF) due to source and processing conditions. These values were in similar ranges of cellulose content of DF from rice bran (8.11–26.11 **g/100g**) subjected to different processing conditions (Liu et al., 2021). HFDF, WSDF and OPDF had the highest cellulose contents whereas AC-APDF, AL-APDF and PSDF had moderate cellulose contents. The cellulose content of rice bran (4.39–6.78 **g/100g**) varied due to differences in processing treatments between defatted and full-fat samples (Casas et al., 2019). The lignin contents are the non-digestible components of the DF, and it ranged from 2.76 **g/100g** (OPDF) to 43.45 **g/100g** (PSDF). AL-APDF and AC-APDF although from the same source had different lignin contents due to the processing conditions. Alkaline treatment may have cleaved lignin-CHO bonds hence a lower lignin content than the acid treated sample (Chu et al., 2019). The lignin content of rice bran varied significantly across different processing conditions, reflecting the impact of treatment methods on DF composition (Casas et al., 2019; Liu et al., 2021) The differences in the extractives, hemicellulose, cellulose and lignin contents of the various DF samples highlight the impact of source material and processing conditions on fibre composition. The effect of different processing methods was seen to have increased the cellulose, hemicellulose and lignin contents of DF from rice bran (Liu et al., 2021). Fermentation with *Bacillus natto* altered the fibre composition of millet bran, reducing hemicellulose (47.3–44.4 **g/100g**), cellulose (17.3–14.3 **g/100g**), and lignin (8.8–7.9 **g/100g**) (Chu et al., 2019). Similar trends have been seen in rice, wheat, millet and oat bran DF, showing that processing and raw material differences affect fibre composition and functionality (Casas et al., 2019; Chu et al., 2019; Liu et al., 2021).

3.2. Particle size distribution

The particle size distribution is a key parameter in understanding the functional and structural composition of dietary fibres (Ma & Mu, 2016). The particle size distribution of the various dietary fibres are shown in Fig. 3 below and Table 2, results include the D_{10}, D_{50} and D_{90} values, along with the span and volume fraction, providing a comprehensive characterization of particle size.

The particle size distribution shows great variations among the various dietary fibre samples as illustrated in Fig. 3 and Table 2 above. In Fig. 3, MCDF showed a very narrow distribution with the highest volume fraction, indicating uniform particle sizes but limited diversity. Similarly, PSDF and OBDF had narrow peaks and low volume, suggesting fine particles with minimal heterogeneity. In contrast, CSDF and OHDF showed broader distributions and relatively higher volume percentages, indicating more diverse particle sizes. HFDF had the broadest span but the lowest volume fraction, suggesting a highly heterogeneous particle population. The distribution of AC-APDF, OPDF, AL-APDF and WSDF were very similar which were neither too narrow nor extremely broad. The D_{10}, D_{50}, and D_{90} values (Table 2) confirms these observations quantitatively. Notably, there were no significant difference in D_{10} values among samples PSDF, MCDF and OBDF, suggesting comparable fine particle content. However, PSDF and OBDF shared similar D_{50} values, indicating comparable median particle sizes while AL-APDF, AC-APDF and WSDF clustered in D_{50}, suggesting similar mid-range distributions. The D_{90} values were mostly distinct, except for AL-APDF and AC-ADDF, which were statistically similar, aligning with their shared source despite different extraction methods. The span values reinforced these trends, with OBDF and HFDF being similar in breadth, while AL-APDF, AC-APDF, OPDF and WSDF grouped together, indicating consistent moderate distribution widths which were a reflection in their good hydration properties illustrated in Table 3 below. This suggests that optimal functionality requires a balanced particle size distribution, as Ma & Mu, 2016 found that both excessively small (<40 μm) and large (>120 μm) particles exhibited poor hydration properties, a reflection in the WHC and WBC results. Similar to our results, Huang et al., 2021 and separately, Ma & Mu, 2016, reported that while processing affects particle size, smaller particles do not always enhance functionality, highlighting that structural factors may outweigh size in determining hydration and emulsification properties.

3.3. Hydration and oil holding properties of dietary fibres

The hydration capacity of a material is an important parameter that influences the physicochemical, functional, and quality of the material. Various parameters such as WHC, WBC and SC can be used to assess the

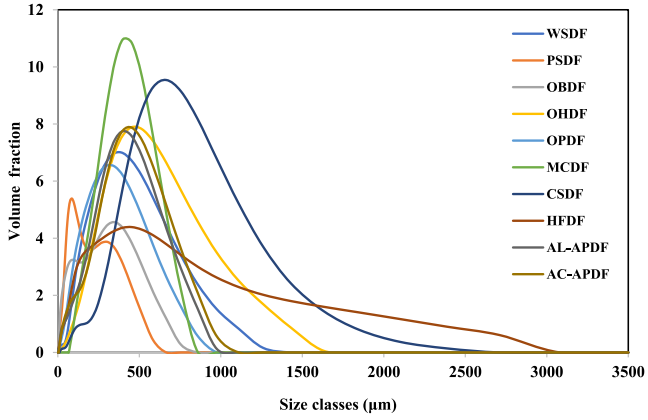

Fig. 3. Particle size distribution chart of the dietary fibre samples obtained from various agri-food by-products sources.

Table 2
Particle size distribution dietary fibres samples from different agri-food by-products.

Sample codes	D_{10} (μm)	D_{50} (μm)	D_{90} (μm)	Span
OBDF	14.70 ± 0.60^{a}	119.33 ± 0.58^{a}	463.67 ± 5.51^{a}	3.76 ± 0.06 ^{a}
HFDF	48.43 ± 0.25^{b}	309.33 ± 2.89^{b}	1183.33 ± 15.28^{b}	3.55 ± 0.06^{a}
AC-APDF	50.10 ± 3.16^{b}	328.33 ± 7.23^{c}	669.67 ± 15.13^{c}	1.89 ± 0.01^{bc}
AL-APDF	46.70 ± 0.26^{b}	319.67 ± 4.04^{bc}	651.33 ± 9.07 ^{cd}	1.89 ± 0.02^{bc}
OHDF	155.67 ± 3.79^{c}	450.67 ± 6.66^{d}	987.33 ± 2.00^{e}	1.80 ± 0.04^{cd}
WSDF	102.33 ± 0.58^{d}	318.33 ± 1.53^{bc}	1.92 ± 1.53^{f}	1.92 ± 0.02^{bc}
PSDF	16.17 ± 3.32^{a}	95.40 ± 5.75^{a}	393.00 ± 5.75^{g}	3.99 ± 0.22^{e}
CSDF	212.67 ± 5.51^{e}	630.00 ± 14.53^{e}	1226.67 ± 14.53^{h}	1.62 ± 0.03^{df}
MCDF	20.30 ± 2.72^{a}	392.33 ± 11.59^{f}	630.67 ± 15.63^{d}	1.56 ± 0.06^{f}
OPDF	61.37 ± 0.91^{f}	237.67 ± 5.03^{g}	556.33 ± 5.03^{i}	2.10 ± 0.03^{c}

NB: all data are means and S.D. of triplicate measurements; different letters denote significant difference in the column at $P < 0.05$. OHDF: oat hulls dietary fibre, WSDF: wheat straw dietary fibre, AL-APDF: alkaline extracted apple pomace dietary fibre, AC-APDF: acid extracted apple pomace fibre, OPDF: onion peels dietary fibre, MCDF: mushroom compost dietary fibre, HFDF: hemp fibre dietary fibre, CSDF: coffee silverskin dietary fibre, OBDF: oat bran dietary fibre, PSDF: pumpkin seed dietary fibre, MC: methylcellulose.

Table 3
Water holding, water binding and swelling capacities of dietary fibre samples from various agri-food by-products sources.

Sample codes	WHC (g/g)	WBC (g/g)	SC (mL/g)	OHC (g/g)
OBDF	2.90 ± 0.17^{a}	0.82 ± 0.01^{a}	2.48 ± 0.33^{b}	1.58 ± 0.06^{a}
HFDF	7.82 ± 0.54^{e}	0.89 ± 0.00^{b}	4.50 ± 1.18^{bcd}	6.76 ± 0.25^{d}
AC-APDF	12.74 ± 0.86^{d}	0.93 ± 0.00^{cd}	6.18 ± 1.04^{cd}	5.61 ± 0.18^{d}
AL-APDF	12.56 ± 0.85^{d}	0.94 ± 0.01^{d}	7.31 ± 1.56^{d}	8.53 ± 0.58^{f}
OHDF	3.58 ± 0.04^{ab}	0.81 ± 0.01^{a}	2.53 ± 0.37^{b}	1.59 ± 0.03^{a}
WSDF	9.63 ± 0.10^{c}	0.91 ± 0.001^{c}	6.34 ± 0.78^{cd}	6.38 ± 0.27^{e}
PSDF	4.40 ± 0.06^{bc}	0.82 ± 0.00^{a}	0.61 ± 0.25^{a}	2.60 ± 0.15^{b}
CSDF	4.98 ± 0.23^{b}	0.86 ± 0.01^{b}	2.97 ± 0.63^{b}	3.07 ± 0.06^{b}
MCDF	3.30 ± 0.04^{ab}	0.82 ± 0.01^{a}	3.02 ± 0.35^{b}	0.86 ± 0.03^{c}
OPDF	11.91 ± 0.41^{d}	0.94 ± 0.01^{d}	13.85 ± 0.45^{e}	1.88 ± 0.09^{a}
MC	12.74 ± 0.42^{d}	0.94 ± 0.01^{d}	4.73 ± 0.73^{bc}	2.22 ± 0.08^{a}

NB: all data are means and S.D. of triplicate measurements; different letters denote significant difference in the column at $P < 0.05$. OHDF: oat hulls dietary fibre, WSDF: wheat straw dietary fibre, AL-APDF: alkaline extracted apple pomace dietary fibre, AC-APDF: acid extracted apple pomace fibre, OPDF: onion peels dietary fibre, MCDF: mushroom compost dietary fibre, HFDF: hemp fibre dietary fibre, CSDF: coffee silverskin dietary fibre, OBDF: oat bran dietary fibre, PSDF: pumpkin seed dietary fibre, MC: methylcellulose.

hydration properties of a material to optimize its processing, formulation, and storage conditions to achieve the desired product quality attributes.

WHC is the amount of water absorbed per gram of sample (Wang et al., 2017). The WHC of the extracted fibres ranged from 2.90 to 12.74 g/g with MC and AC-APDF having the highest and OBDF having the lowest WHC values, respectively. The WHC values obtained for the DF were in the ranges similar to WHC values of some agriculture by-products from rice hull (2.58 g/g), malt bagasse (3.68 g/g), fibrous residue from banana pseudo-stems (4.71 g/g) (Jacometti et al., 2015); maize hulls (2.32 g/g), wheat hulls (2.48 g/g) (Zambrano et al., 2001); alkaline extracted flax seed gum (4.85 g/g), enzyme extracted flaxseed gum (6.35 g/g) (Moczkowska et al., 2019); papaya peel (4.93 g/g) (Zhang et al., 2017). There were no significant differences at $p < 0.05$ observed for the WHC values of AL-APDF, AC-APDF, OPDF and MC. AL-APDF, AC-APDF, MC and OPDF recorded WHC values of >10.0 g/g while all other samples recorded WHC values of <10.0 g/g. According to previous studies, the WHC of DF are primarily influenced by a number of factors including their soluble dietary fibre to insoluble dietary fibre ratio, microstructure of the samples, surface of area of the material, particle size distribution and the presence of hydrophilic sites (Jacometti et al., 2015; Zhang et al., 2017; Zou et al., 2022). The DF samples with more porous microstructures, and a more balanced particle size distribution tend to have a relatively higher WHC value than the other DF samples (Fig. 7). The samples with extremely narrow and extremely broad particle size distribution had relatively poor WHC values.

WBC, i.e. the ability of the material to hold water molecules in its structure when subjected to stress conditions, is a very important physicochemical properties that defines the usefulness of a food material in food processing. The WBC of the various DF samples ranged from 0.82 to 0.94 g/g. The WBC values were lower than some DF obtained from different types of mushroom Sclerotia (2.72–6.66 g/g)(Wong & Cheung, 2005); IDF from wheat bran (3.2–4.4 g/g) (Liao et al., 2022); DF from de-oiled cumin extracted using different methods and of different particle sizes (3.30 g/g to 7.28 g/g) (Ma & Mu, 2016); and DF from black rice bran (6.30–8.15 g/g) (Zhang et al., 2024). The samples that showed the potential of having similar water binding properties as MC included OPDF, AL-APDF and AC-APDF with no significant differences at $p < 0.05$ being observed between their WBC. The samples (OPDF, MC, AL-APDF, AC-APDF and WSDF) with relatively lower moisture content as displayed in Table 1 and moderately uniform particle size distribution with balanced volume, indicating a well-distributed profile that supported a relatively higher WBC content. This could be because of more free and available hydroxyl groups in these samples to bind with water (Zou et al., 2022).

The SC of DF refers to the volume of fully hydrated fibre per gram of initial material, and is influenced by factors such as surface area, particle size, molecular structure, fibre composition, and porosity. OPDF and PSDF had the highest (13.85 mL/g) and lowest (0.61 mL/g) SC values, respectively, and were significantly different at $p < 0.05$ from all the other samples. There were no significant differences observed for the SC values of MC, MCDF, CSDF, OHDF, HFDF, and OBDF. The SC values of the DF samples were in the same range as the SC values of fibrous components from pear pomace (3.10–7.89 mL/g) (Yan et al., 2019); apple pectin (6.51 mL/g) (Gouw et al., 2017); malt bagasse (4.53 mL/g), rice hull (3.27 mL/g), fibrous residue from banana pseudo-stems (4.98 mL/g) (Jacometti et al., 2015); and orange soluble DF (2.03 mL/g) (Zou et al., 2022). However, all SC values were lower than the SC values reported for psyllium arabinoxylan (14.38 mL/g) and flaxseed soluble DF (15.52 mL/g) (Zou et al., 2022). The varying range of SC amongst the fibres could be attributed to the different chemical composition of the DF samples, the microstructure of the DF as well as the extraction method properties (Gouw et al., 2017; Zou et al., 2022). Fig. 7 below shows the different microstructure of the DF, with OPDF and AL-APDF having a more porous surface with more pore spaces which enabled them to trap more water and increase their SC.

There were no significant differences at $p < 0.05$ in the OHC values of OBDF, OHDF, OPDF and MC. However, there were significant differences observed between MC and the other sources of DF. AL-APDF had the highest OHC with a value of 8.53 g/g and MCDF recorded the lowest OHC value of 0.86 g/g. The OHC of DF are determined by its hydrophobicity, charge density, extraction conditions, nature of

materials and surface properties (Kuan et al., 2011; Moczkowska et al., 2019; Yan et al., 2019). The OHC values for the various DF samples were within the same range of OHC of soluble DF from flaxseed (Moczkowska et al., 2019); rice hull (1.85 g/g), malt bagasse (2.46 g/g) (Jacometti et al., 2015); pear pomace (1.15–1.40 g/g) (Zhang et al., 2017). The OHC of DF from pear pomace was reported to be affected by the extraction methods with high pressure extracted DF having a higher OHC value as compared to super fine grinding (Yan et al., 2019). Also, ultrasound-alkaline assisted extraction was reported to have enhanced the OHC property of DF from pear pomace as compared to alkaline extraction only (Zhang et al., 2017). Kuan et al. (2011) reported that the type of raw material influenced the OHC value of DF extracted from corn cob and wheat straw with corn cob having a relatively higher OHC value than wheat straw.

Following the study of the basic physiochemical parameters, it was necessary to consider their impact on the emulsifying properties of DF as hydration plays an important role on how DF stabilises and enhances emulsions.

3.4. Emulsifying properties (emulsion capacity and stability)

The DF samples were studied for their emulsifying capacity (EC) and emulsion stability (ES) to evaluate their functionality further. ES refers to the ability of a molecule to maintain an emulsion and its resistance to rupture, whereas EC refers to its ability to facilitate the solubilisation of immiscible liquids.

Fig. 4 shows the emulsion capacity and emulsion stability of the various DF samples. The EC values ranged from 0.00 to 44.41 mL/mL with MC having the lowest EC value and OBDF having the highest EC value. The lower the EC value the better the emulsion formed. The fibre samples with the lowest EC values showing a potential as good emulsifiers <20 mL/mL included OPDF (12.04 mL/mL) and AL-APDF (17.08 mL/mL); these could act as decent emulsifiers in formulated foods. However, samples such as MCDF, PSDF, HFDF, WSDF, CSDF, OHDF and OBDF showed no emulsifying potential. This is because these samples lack sufficient hydrophobic and hydrophilic regions causing an imbalance, hence, not being able to stabilise the two interfaces (oil and water). These samples demonstrated relatively lower WHC and OHC values. DF

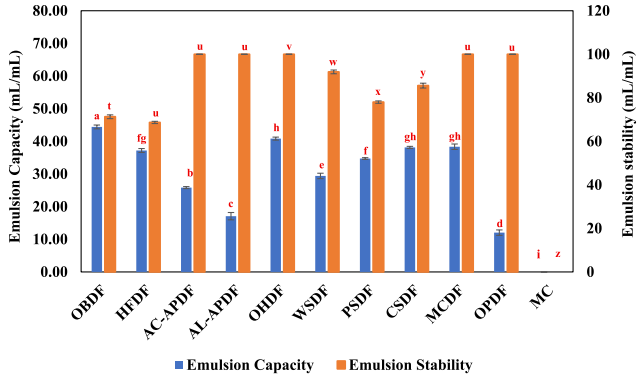

Fig. 4. Emulsifying capacity and stability of the various DF samples.
OHDF: oat hulls dietary fibre, WSDF: wheat straw dietary fibre, AL-APDF: alkaline extracted apple pomace dietary fibre, AC-APDF: acid extracted apple pomace fibre, OPDF: onion peels dietary fibre, MCDF: mushroom compost dietary fibre, HFDF: hemp fibre dietary fibre, CSDF: coffee silverskin dietary fibre, OBDF: oat bran dietary fibre, PSDF: pumpkin seed dietary fibre, MC: methylcellulose. Statistical significance is indicated separately for each experiment. For emulsion capacity (blue bars), different letters (a–h) denote significant differences in the graph at $p < 0.05$. For emulsion stability (orange bars), different letters (t–z) denote significant differences in the graph at $p < 0.05$. The error bars. For each analysis, the error bars represent the standard error of the means from three independents replicates for each sample.

with good WHC and OHC have been reported to form stable emulsions as they are able to bridge the two interfaces together and prevent phase separation (Huang et al., 2021). MCDF and PSDF lacked emulsifying capacity despite moderate heat-to-temperature ratios, a condition that typically enhances functionality in biopolymers. This suggests that heat to temperature ratio alone may not determine emulsification performance. Beyond thermal effects, protein interfacial behaviour plays a significant role in emulsification. Proteins are well-known surface-active agents due to their ability to adsorb at oil–water interfaces and stabilise emulsions (Murray et al., 2011). Despite the relatively high protein contents of MCDF (33.46 g/100g) and PSDF (11.44 g/100g), their poor emulsifying properties may have resulted from structural or functional constraints of the proteins, such as denaturation, aggregation, or interactions with non-protein components, which may have hindered their interfacial activity. In addition, while some plant polysaccharides, such as sugar beet pectin and gum arabic, contain amphiphilic groups that aid in adsorption at oil–water interfaces (Bai et al., 2017), MCDF and PSDF may have had limited surface activity or insufficient amphiphilicity to effectively lower interfacial tension. Similarly, corn fibre gum has been reported to show poor emulsification due to slow interfacial adsorption, a lack of amphiphilic groups, and an unfavourable molecular structure (Bai et al., 2017). MC had the best EC as no emulsion layer was observed and the stability of the emulsion was not altered, with no sign of serum layer after heating.

The ES of the prepared emulsions under heating conditions was also evaluated. The emulsion serum of some samples remained the same after heating. MC remained the same with no emulsion layer forming, as MC is an excellent emulsifier, showing no separation after heating and centrifugation. The EC of MC was significantly different from all DF samples. However, it was comparable to the EC values of soluble DF obtained from nodes of lotus root (0.17–0.47 mL/mL) (Chen et al., 2018) and higher than EC values of corn cob DF (0.0373 mL/mL), WSDF (0.0529 mL/mL) (Kuan et al., 2011); and DF from tiger nut by-products (0.7033 mL/mL) (Sánchez-Zapata et al., 2009). The emulsions made with OPDF, MCDF, AL-APDF, AC-APDF and OHDF had an ES value of 100 mL/mL with no changes in the serum layer before and after heating. The samples with the lowest ES were OBDF, PSDF and HFDF and also had relatively poor EC values. The ES of all samples except OBDF, PSDF and HFDF were higher the ES values of corn cob DF (80 mL/mL) (Kuan et al., 2011) and peanut shell DF (66.37–79.69 mL/mL) (Wang et al., 2023). However, the ES values of OPDF, MCDF, AL-APDF, AC-APDF and OHDF were similar to ES values of DF from tiger nut by-products (Sánchez-Zapata et al., 2009) and passion fruit (Selvamuthukumaran & Shi, 2017). DF with high ES values (100 mL/mL) is an indication that they could act as good emulsifiers in foods such as plant-based confectionery, beverages, sauces, and other processed food products that require stabilisation of emulsions for an extended period of time (Kuan et al., 2011). However, although useful, emulsifying properties alone do not give a full picture on the DF's functional and structural performance in a food system and therefore, rheological investigation was necessary.

3.5. Rheological properties

3.5.1. Apparent viscosity

A steady shear experiment was used to understand the flow behaviour of the DF samples in a solution.

As shown in Fig. 5, the apparent viscosity of all samples decreased with increasing shear rates at 25 °C exhibiting a shear thinning behaviour. Similar behaviours were observed for soluble DF from flaxseed (Moczkowska et al., 2019), orange, psyllium seed, soybean, oat glucan, konjac glucomannan, and apple pectin (Zou et al., 2022), and node of lotus root (Chen et al., 2018). At lower shear rates the order of viscosity for the DF fibres were OPDF > HFDF > WSDF > AL-APDF > OHDF > AC-APDF > MC > CSDF > OBDF > PSDF. MC, AL-APDF, AC-APDF, WSDF, OPDF, HFDF, and OHDF observed a sharp decrease in their viscosity with increasing shear rates with a higher apparent viscosity above

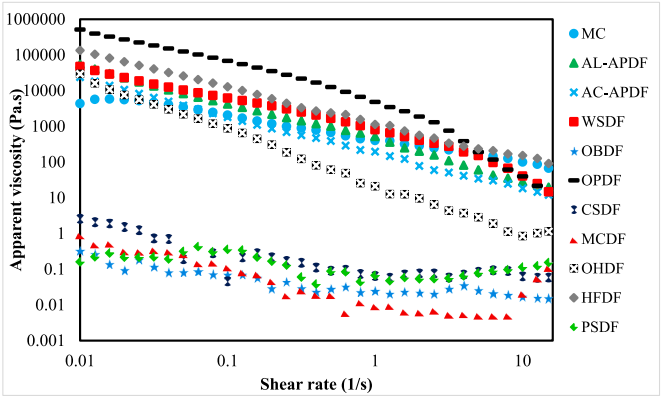

Fig. 5. Effect of increasing shear rate of the viscosity of DF samples.
Notes: OHDF: oat hulls dietary fibre, WSDF: wheat straw dietary fibre, AL-APDF: alkaline extracted apple pomace dietary fibre, AC-APDF: acid extracted apple pomace fibre, OPDF: onion peels dietary fibre, MCDF: mushroom compost dietary fibre, HFDF: hemp fibre dietary fibre, CSDF: coffee silverskin dietary fibre, OBDF: oat bran dietary fibre, PSDF: pumpkin seed dietary fibre, MC: methylcellulose.

1000 Pa s as compared to the other DF samples. PSDF, OBDF, MCDF and CSDF observed the lowest apparent viscosity <100 Pa s with increasing shear rate. Peanut shells derived DF from various extraction methods exhibited shear thinning behaviours with apparent viscosity values < 100 Pa s (Wang et al., 2023). MCDF and PSDF exhibited shear thinning behaviour as the shear rate was increasing and changed to a shear thickening behaviour at a shear rate of 10/s. MCDF and PSDF exhibited poor WHC, WBC, and SC properties, which may be indicative of their hydrophobic nature. At high shear rates, hydrophobic interactions and hydrogen bonding among polysaccharide chains may have intensified due to the forced proximity of molecules, promoting transient associations that may have increased resistance to flow. These interactions may have caused the polysaccharide chains to temporarily stick or cluster, making the mixture thicker and contributing to the observed shear thickening behaviour. Additionally, the presence of insoluble fibre fractions, possibly characterised by a high lignin content in PSDF, may have led to the formation of temporary physical networks. As shear compressed these particles into closer contact, they may have formed dynamic structures that resisted deformation. This combination of molecular interactions and physical entanglement may have contributed to the increased viscosity under shear. Likewise, OBDF and CSDF observed a steady increase and decrease in their viscosity with increasing shear rate. There was not a stable observation in terms of their flow behaviour.

3.5.2. Temperature sweep

Temperature sweep tests were carried out on all DF suspensions to characterize the viscoelastic behaviour as a function of temperature.

Fig. 6 shows how each DF behaves with increasing temperature. MC the standard had both storage modulus (G′) and loss modulus (G″) increasing sharply with increasing temperature, with initial G′ and G″ values of around 1000 Pa. Aside MC, other DF suspensions such as PSDF, CSDF, and MCDF exhibited similar behaviour with an increasing G′ and G″ values with increasing temperature. However, their initial G′ and G″ values were <100 Pa and the final values were ≤1000 Pa. These fibres had initially a lower degree of viscosity, but with increasing temperature the viscosities increased making the material resistant to deformation and dissipating a significant amount of energy as heat under stress conditions. The observation of an increase in both loss and storage moduli with increasing temperature suggests a complex thermal response of the DF, possibly associated to changes in structural transitions, intermolecular interactions, or molecular mobility (Chen et al., 2018). WSDF, HFDF, OPDF, AL-APDF and AC-APDF although had relatively higher initial G′ and G″ values, the dispersions observed a

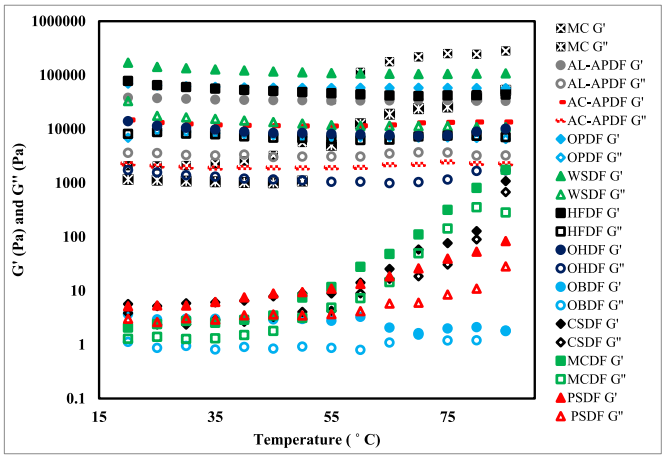

Fig. 6. Effect of temperature on viscosity of DF samples. *OHDF: oat hulls dietary fibre, WSDF: wheat straw dietary fibre, AL-APDF: alkaline extracted apple pomace dietary fibre, AC-APDF: acid extracted apple pomace fibre, OPDF: onion peels dietary fibre, MCDF: mushroom compost dietary fibre, HFDF: hemp fibre dietary fibre, CSDF: coffee silverskin dietary fibre, OBDF: oat bran dietary fibre, PSDF: pumpkin seed dietary fibre, MC: methylcellulose.*

different behaviour to the standard (MC) were their G′ and G″ values decreased slightly with increasing temperature. Similarly, Chen et al. (2018) observed that the viscosity of soluble DF from nodes of lotus root decreased as the temperature increased.

3.6. Structural analysis

3.6.1. Scanning electron microscopy

The microstructure of DF is an important characteristic that influences the functional properties of a material such as the WHC, WBC, SC and its interaction with other components (Zou et al., 2022). This is essential to understand the impact on the hydration and solubility properties of DF and its interaction with water, oil and other molecules present.

The various microstructures of the fibres are displayed in Fig. 7 and all samples showed distinct structures. AC-APDF displayed a flakier structure with quite a smooth and porous structure. AL-APDF on the hand had a loose, smoother, and porous structure with a wide surface area indicating it would be easier to form a network structure with water molecules, which was evident in its hydration and other physicochemical properties. Fidriyanto et al. (2023) observed acid extracted apple pomace to have a porous structure with aggregated irregular smooth layer and cavities on the outer surface as compared to alkali extracted apple pomace. Also, steam explosion extracted apple pomace fibres presented loose and crumbled surfaces with a several holes (Liang et al., 2018). CSDF had a flaky particle structure with no pores and a flatter surface. CSDF's non-porous, and flat surface limited water penetration and reduced available surface area for interaction, leading to poor hydration properties. This morphology also hindered emulsifying capacity due to fewer active sites at the interface. Additionally, limited water uptake and structural rigidity contributed to its low apparent viscosity by restricting network formation in dispersion. HFDF displayed a long and fibrous structure resembling threads with varying length and uniform thickness. The surface appeared as textured with irregularities making it look like a cluster of fibre bundles with a hierarchical structure, loose surface and concentric layers. MCDF had particles with a roundish structure and with relatively cleaner and smaller particle sizes which contrasts with the observation made by Wong and Cheung (2005); the microstructure of three different species of mushrooms presented fragments of interwoven hyphae, and the number of hyphae was different for each species. OBDF exhibited a loose stacked smaller particle with a compact and a non-porous structure. OHDF and WSDF

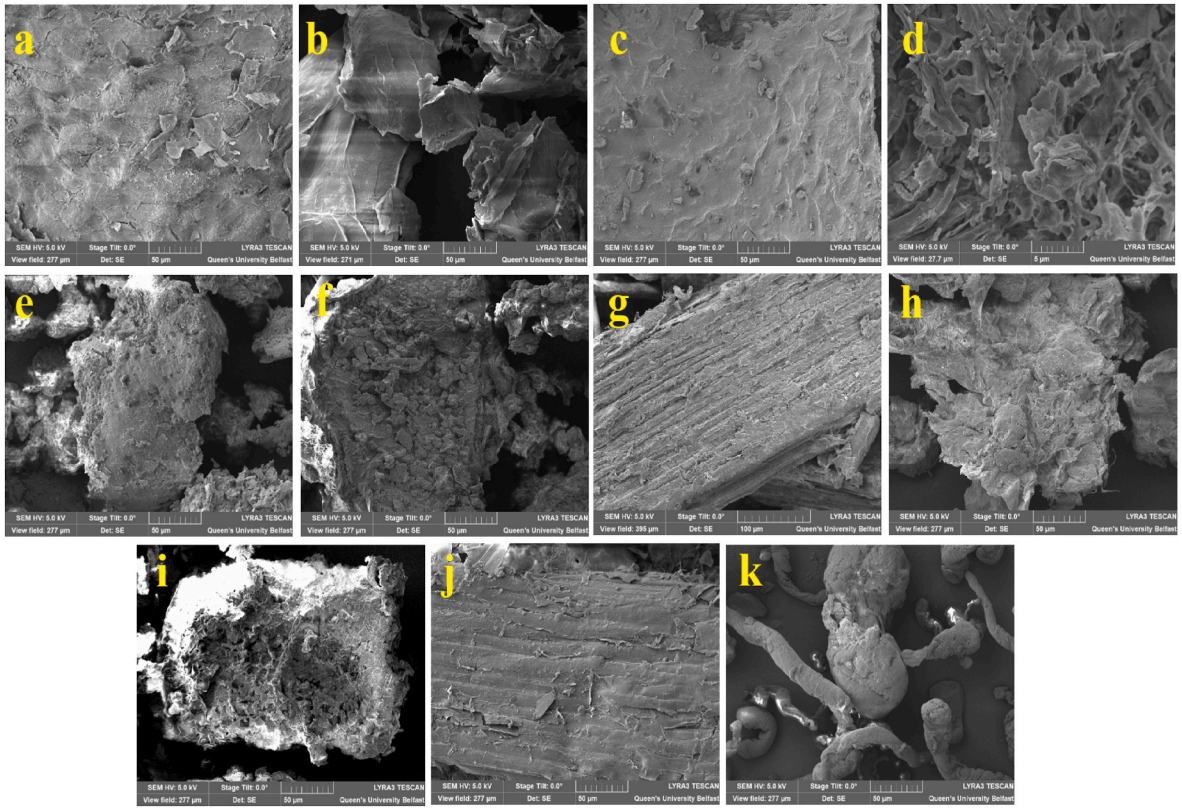

Fig. 7. Scanning electron micrographs of (a) acid extracted dietary fibre from apple pomace (AC-APDF) (b) alkaline extracted dietary fibres from apple pomace (AL-APDF) (c) coffee silver skin dietary fibres (CSDF) (d) hemp fibre dietary fibres (HFDF) (e) mushroom dietary fibres (MCDF) (f) oat bran dietary fibres (OBDF) (g) oat hulls dietary fibres (OHDF) (h) onion peels dietary fibres (OPDF) (i) pumpkin seeds dietary fibres (PSDF) (j) wheat straw dietary fibres (WSDF) (k) methylcellulose (MC). Scale provided in each picture in μm.

showed similarities in their microstructure, as both fibres had irregularly shaped flakes of uneven sizes and a dense surface with smaller particles on the surfaces. In contrast, alkali extracted wheat straw nanofibers showed a coarse and flaky surface (Kuan et al., 2011). OPDF showed a highly irregular structure consisting of small and clean particles separated by small pores which enhanced water penetration and surface interaction. This porous morphology likely promoted better hydration, emulsification, and viscosity by increasing water uptake, swelling capacity, and molecular entanglement, leading to improved overall functional properties. PSDF densely packed, small particles with a compact, stacked-plate morphology restricted water accessibility and surface area, resulting in limited hydration, reduced emulsification efficiency, and lower rheological performance. MC, which is the standard, displayed long chains that appear interconnected with fibrous structures of varying length and thickness unevenly disperse. MC had a textured appearance that was characterised by roughness, irregularities and cluster forming chains.

3.6.2. FTIR

FTIR (Fourier Transform Infrared) spectroscopy analysis was conducted to compare and identify the molecular structural differences, chemical compositions and the functional groups present in the different DF. This helps us to understand the molecular bonds present and predict their interactions within a food matrix.

A characteristic absorption peak for cellulose polysaccharides was observed in all DF samples. The FT-IR spectra of all DF samples showed a broad stretching characteristic peak at around 3400 cm^{-1} as seen in Fig. 8 indicating the presence of stronger intermolecular hydrogen forces, which were attributed to O–H the stretching vibration of hemicellulose (Jacometti et al., 2015). The hydroxyl stretching vibration of cellulose and hemicellulose occurred at around 3419 cm^{-1}, while the

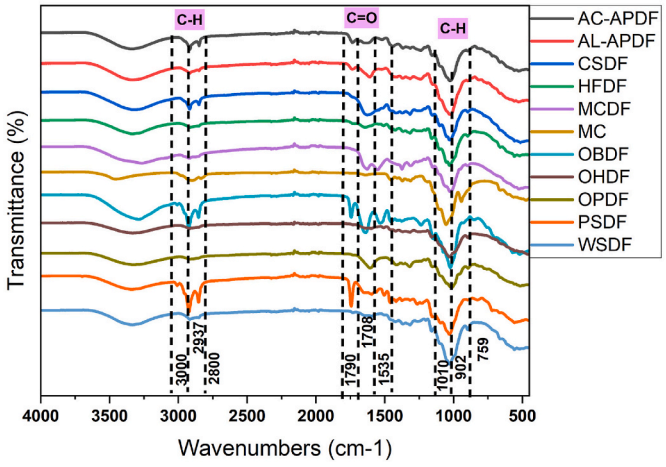

Fig. 8. Infrared spectroscopy of dietary fibres obtained from various agri-food by-products samples. *OHDF: oat hulls dietary fibre, WSDF: wheat straw dietary fibre, AL-APDF: alkaline extracted apple pomace dietary fibre, AC-APDF: acid extracted apple pomace fibre, OPDF: onion peels dietary fibre, MCDF: mushroom compost dietary fibre, HFDF: hemp fibre dietary fibre, CSDF: coffee silverskin dietary fibre, OBDF: oat bran dietary fibre, PSDF: pumpkin seed dietary fibre, MC: methylcellulose.*

vibration of cellulose -CH and -CH_2 occurred at 2800-3000 cm^{-1} (Kanwar et al., 2023; Zou et al., 2022). The peak intensity for hydroxyl stretching vibration of cellulose and hemicellulose was more prominent in OBDF, WSDF, CSDF, AL-APDF and AC-APDF. While hydroxyl groups are generally associated with hydrophilicity due to their ability to form

hydrogen bonds with water, the poor water-holding and swelling capacities observed in OBDF and CSDF suggest that these –OH groups may be embedded within highly ordered structures, limiting their accessibility and interaction with water. This structural constraint may have also negatively influenced other physicochemical properties, such as apparent viscosity, emulsifying ability, and oil holding capacity, by reducing the fibres' surface activity and interaction with surrounding media. In addition, the C–H and $–CH_2$ stretching vibrations, particularly intense in PSDF, OBDF, and CSDF, may indicate a greater presence of non-polar or structurally rigid components, such as crystalline cellulose or lignin-rich regions. This interpretation is supported by our compositional data, which showed that PSDF and CSDF had relatively higher lignin contents, while OBDF exhibited a higher hemicellulose content. Although hemicellulose contains some hydrophilic groups, it is often embedded within complex fibre matrices, and its functionality can be influenced by its structural arrangement and interactions with lignin or cellulose. The combined presence of lignin and rigid polysaccharide structures in these samples may have contributed to reduced surface activity and molecular flexibility, thereby limiting their physicochemical activities. The absorption peak near 1535 cm^{-1} was assigned as the stretching vibration absorption of the aromatic hydrocarbons in lignin (Vârban et al., 2021). The absorption peak near 1620 cm^{-1} corresponded to the characteristic absorption of the C=O bond in uronic acid present in hemicellulose and pectin (Chu et al., 2019). From the spectra, it shows that MC had no peak around 1620 cm^{-1} likewise WSDF, HFDF and OHDF. The peak between 1000 and 1200 cm^{-1} is indicative of C-O stretching vibrations of sugar rings of cellulose and hemicellulose corresponding to the presence of C-O-C and C-O-H (Zhang et al., 2017). The peaks in the range of 759–1010 cm^{-1} are indicative of the presence of α- and β-pyranose, furanose, and β-glucoside bond which were characteristic in all DF samples (Xie et al., 2017).

3.7. Multivariate pattern recognition analysis

Principal Component Analysis (PCA) as applied to explore the correlation between the various DF samples and MC (standard) as shown in Fig. 9.

The first and second principal component (PC) explained 57.8 and 26.2 parts per hundred respectively of the total variables with a total of three clusters, cluster1; MC, AL-APDF, AC-APDF, WSDF and HFDF, cluster 2; OBDF, OHDF, CSDF, MCDF, and PSDF cluster 3; OPDF forming a single cluster. From the score plot, MC, AL-APDF, AC-APDF, WSDF and HFDF were correlated positively to PC 1 axis. OBDF, OHDF, CSDF, MCDF and PSDF formed a cluster and were positively correlated to PC2 axis, whilst OPDF was negatively correlated to PC2 axis. The cluster formed by OBDF, OHDF, CSDF, MCDF and PSDF were not correlated to PC1 axis. Therefore, these samples were not associated with OHC, WBC, WHC and SC. This correlates with the observations made in the WHC, WBC, OHC and SC analysis where these samples did not meet the expected physicochemical and functional properties. This indicates that

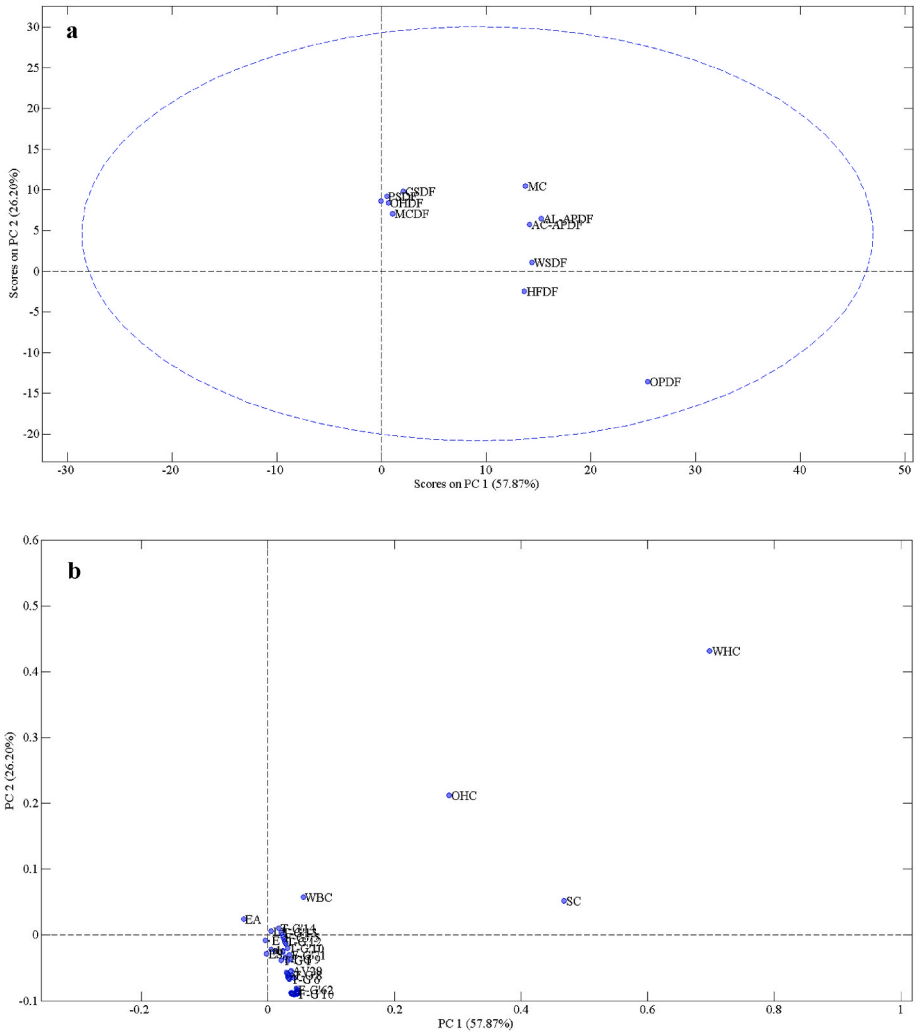

Fig. 9. Principal component analysis of extracted dietary fibres from various agri-food by-products: (A) PCA scores plot highlighting sample groupings (B) PCA loading plot identifying key contributing variables.

these samples were like each other in terms of their functionalities but were different from the standard MC. The loading plot shows that certain properties (WHC, OHC,WBC, SC) strongly influence the main differences in our data, grouping samples with similar properties closely together. The rheological parameters including the apparent viscosity values were negatively correlated to PC2, whilst OHC, WBC, WHC and SC were positively correlated to PC1 and PC2 axes. According to the PCA results the physicochemical and rheological properties of the different fibres were distinctively different. The PCA results appeared to be consistent with the results of the physicochemical properties discussed earlier.

4. Conclusions

The findings from the study show that the physicochemical and rheological properties vary for each DF and the type of extraction may influence the functionalities. While method-dependent differences exist, we identified which by-product and method combinations optimize specific functional properties. This enables targeted selection of extraction approaches for sustainable valorisation. MC, AL-APDF, AC-APDF and OPDF showed the highest WHC, WBC, and SC values. The findings suggest that MC exhibited the highest emulsifying and stabilizing capacity, OPDF, AC-APDF and AL-ACDF also showed potential in these properties. The differences in microstructure were likely influenced by composition and extraction methods leading to variations in the rheological properties. Notably, all extracted DF samples displayed shear-thinning properties, highlighting the impact of structural and compositional factors in their functionality. The variations in peak positions observed in the FT-IR spectra indicate differences in the chemical composition of the samples, highlighting the presence of distinct functional groups. The correlation analysis results appeared to be consistent with the results from the physicochemical analysis of the samples and suggests a positive correlation between MC, AL-APDF, AC-APDF, WSDF and HFDF samples associated with properties such as WBC, WHC, SC and OHC. The variations in results for each property is an indication of how processing techniques and raw materials sources play a useful role in altering the physicochemical and functional properties of a material. Understanding the composition of DF is important for determining the appropriate applications of each DF, whether as functional ingredient in food, feed, pharmaceutical or non-food applications.

CRediT authorship contribution statement

Whitney Vale-Hagan: Writing – original draft, Methodology, Investigation, Formal analysis, Data curation. **Dimitris Charalampopoulos:** Writing – review & editing, Supervision, Funding acquisition, Conceptualization. **Eoin Cunningham:** Writing – review & editing, Supervision, Resources, Methodology. **Eric Whale:** Writing – review & editing, Resources. **Anastasios Koidis:** Writing – review & editing, Validation, Supervision, Resources, Project administration, Funding acquisition, Conceptualization.

Data availability statement

The original contributions presented in the study are included in the article, further inquiries can be directed to the corresponding author.

Declaration of competing interest

The authors declare that they have no known competing financial interests or personal relationships that could have appeared to influence the work reported in this paper.

Acknowledgments

This research is funded by the UKRI BBSRC doctoral training grant no: BB/T008776/1. The authors extend their deepest appreciation to the funding body for their belief in our project and their commitment to advancing research in the field of Agri-Food Systems. The author would also like to acknowledge the FoodBiosystems DTP.

Data availability

Data will be made available on request.

References

Abolore, R., Jaiswal, S., & Jaiswal, A. (2024). Green and sustainable pretreatment methods for cellulose extraction from lignocellulosic biomass and its applications: A review. *CARBOHYDRATE POLYMER TECHNOLOGIES AND APPLICATIONS, 7*, Article 100396. https://doi.org/10.1016/j.carpta.2023.100396

AOAC. (2016). *Association of official analytical chemists international, official methods of analysis* (20th ed.). Rockville, MD, USA: AOAC International.

Bai, L., Huan, S., Li, Z., & McClements, D. J. (2017). Comparison of emulsifying properties of food-grade polysaccharides in oil-in-water emulsions: Gum Arabic, beet pectin, and corn fiber gum. *Food Hydrocolloids, 66*, 144–153. https://doi.org/10.1016/j.foodhyd.2016.12.019

Casas, G. A., Lærke, H. N., Bach Knudsen, K. E., & Stein, H. H. (2019). Arabinoxylan is the main polysaccharide in fiber from rice coproducts, and increased concentration of fiber decreases in vitro digestibility of dry matter. *Animal Feed Science and Technology, 247*, 255–261. https://doi.org/10.1016/j.anifeedsci.2018.11.017

Chen, H., Xiong, M., Bai, T. M., Chen, D. W., Zhang, Q., Lin, D. R., Liu, Y. T., Liu, A. P., Huang, Z. Q., & Qin, W. (2021). Comparative study on the structure, physicochemical, and functional properties of dietary fiber extracts from quinoa and wheat. *Lwt-Food Science and Technology, 149*, Article 111816. https://doi.org/10.1016/j.lwt.2021.111816

Chen, H., Zhao, C., Li, J., Hussain, S., Yan, S., & Wang, Q. (2018). Effects of extrusion on structural and physicochemical properties of soluble dietary fiber from nodes of lotus root. *LWT, 93*, 204–211. https://doi.org/10.1016/j.lwt.2018.03.004

Chu, J., Zhao, H., Lu, Z., Lu, F., Bie, X., & Zhang, C. (2019). Improved physicochemical and functional properties of dietary fiber from millet bran fermented by bacillus natto. *Food Chemistry, 294*, 79–86. https://doi.org/10.1016/j.foodchem.2019.05.035

Dong, Y. F., Li, Q., Guo, Y. H., Zhao, Y. H., & Cao, J. X. (2023). Comparison of physicochemical and *In Vitro* hypoglycemic activity of bamboo shoot dietary fibers from different regions of Yunnan. *Frontiers in Nutrition, 9*, Article 1102671. https://doi.org/10.3389/fnut.2022.1102671

Eren, N. M., Santos, P. H. S., & Campanella, O. (2015). Mechanically modified xanthan gum: Rheology and polydispersity aspects. *Carbohydrate Polymers, 134*, 475–484. https://doi.org/10.1016/j.carbpol.2015.07.092

Feng, S., Yi, J., Ma, Y., & Bi, J. (2023). The role of amide groups in the mechanism of acid-induced pectin gelation: A potential pH-sensitive hydrogel based on hydrogen bond interactions. *Food Hydrocolloids, 141*, Article 108741. https://doi.org/10.1016/j.foodhyd.2023.108741

Fidriyanto, R., Singh, B. P., Manju, K. M., Widyastuti, Y., & Goel, G. (2023). Multivariate analysis of structural and functional properties of fibres from Apple pomace using different extraction methods. *Food Production, Processing and Nutrition, 5*(1), 6. https://doi.org/10.1186/s43014-022-00119-8

Gouw, V. P., Jung, J., & Zhao, Y. Y. (2017). Functional properties, bioactive compounds, and *In Vitro* gastrointestinal digestion study of dried fruit pomace powders as functional food ingredients. *Lwt-Food Science and Technology, 80*, 136–144. https://doi.org/10.1016/j.lwt.2017.02.015

Guo, Y., Byambasuren, K., Liu, X. X., Wang, X. P., Qiu, S., Gao, Y. J., & Wang, Z. Z. (2021). Extraction, purification, and characterization of insoluble dietary fiber from oat bran. *Transactions of Tianjin University, 27*(5), 385–393. https://doi.org/10.1007/s12209-019-00224-9

Huang, J. Y., Liao, J. S., Qi, J. R., Jiang, W. X., & Yang, X. Q. (2021). Structural and physicochemical properties of pectin-rich dietary fiber prepared from citrus peel. *Food Hydrocolloids, 110*, Article 106140. https://doi.org/10.1016/j.foodhyd.2020.106140

Jacometti, G. A., Mello, L., Nascimento, P. H. A., Sueiro, A. C., Yamashita, F., & Mali, S. (2015). The physicochemical properties of fibrous residues from the agro industry. *Lwt-Food Science and Technology, 62*(1), 138–143. https://doi.org/10.1016/j.lwt.2015.01.044

Jia, F., Liu, X., Gong, Z., Cui, W., Wang, Y., & Wang, W. (2020). Extraction, modification, and property characterization of dietary fiber from Agrocybe cylindracea. *Food Sci Nutr, 8*(11), 6131–6143. https://doi.org/10.1002/fsn3.1905

Kanwar, P., Yadav, R. B., & Yadav, B. S. (2023). Cross-linking, carboxymethylation and hydroxypropylation treatment to sorghum dietary fiber: Effect on physicochemical, micro structural and thermal properties. *International Journal of Biological Macromolecules, 233*, Article 123638. https://doi.org/10.1016/j.ijbiomac.2023.123638

Kuan, C.-Y., Yuen, K.-H., Bhat, R., & Liong, M.-T. (2011). Physicochemical characterization of alkali treated fractions from corncob and wheat straw and the production of nanofibres. *Food Research International, 44*(9), 2822–2829. https://doi.org/10.1016/j.foodres.2011.06.023

Lan, G. S., Chen, H. X., Chen, S. H., & Tian, J. G. (2012). Chemical composition and physicochemical properties of dietary fiber from *Polygonatum odoratum* as affected

by different processing methods. *Food Research International, 49*(1), 406–410. https://doi.org/10.1016/j.foodres.2012.07.047

Liang, X., Ran, J., Sun, J., Wang, T., Jiao, Z., He, H., & Zhu, M. (2018). Steam-explosion-modified optimization of soluble dietary fiber extraction from Apple pomace using response surface methodology. *CyTA-Journal of Food, 16*(1), 20–26.

Liao, A., Zhang, J., Yang, Z., Huang, J., Pan, L., Hou, Y., Li, X., Zhao, P., Dong, Y., Hu, Z., & Hui, M. (2022). Structural, physicochemical, and functional properties of wheat bran insoluble dietary fiber modified with probiotic fermentation. *Frontiers in Nutrition, 9*, Article 803440. https://doi.org/10.3389/fnut.2022.803440

Liu, J., Wang, Z. W., Wang, Z. Y., Hao, Y. M., Wang, Y., Yang, Z. H., Li, W. X., & Wang, J. (2020). Physicochemical and functional properties of soluble dietary fiber from different colored quinoa varieties (*Chenopodium quinoa* willd). *Journal of Cereal Science, 95*, Article 103045. https://doi.org/10.1016/j.jcs.2020.103045

Liu, Y., Zhang, H., Yi, C., Quan, K., & Lin, B. (2021). Chemical composition, structure, physicochemical and functional properties of rice bran dietary fiber modified by cellulase treatment. *Food Chemistry, 342*, Article 128352. https://doi.org/10.1016/j.foodchem.2020.128352

López-Marcos, M. C., Bailina, C., Viuda-Martos, M., Pérez-Alvarez, J. A., & Fernández-López, J. (2015). Properties of dietary fibers from agroindustrial coproducts as source for fiber-enriched foods. *Food and Bioprocess Technology, 8*(12), 2400–2408. https://doi.org/10.1007/s11947-015-1591-z

Lu, X., Chen, J., Guo, Z., Zheng, Y., Rea, M. C., Su, H., Zheng, X., Zheng, B., & Miao, S. (2019). Using polysaccharides for the enhancement of functionality of foods: A review. *Trends in Food Science & Technology, 86*, 311–327. https://doi.org/10.1016/j.tifs.2019.02.024

Luo, X. L., Wang, Q., Fang, D. Y., Zhuang, W. J., Chen, C. H., Jiang, W. T., & Zheng, Y. F. (2018). Modification of insoluble dietary fibers from bamboo shoot shell: Structural characterization and functional properties. *International Journal of Biological Macromolecules, 120*, 1461–1467. https://doi.org/10.1016/j.ijbiomac.2018.09.149

Luo, X., Wang, Q., Zheng, B., Lin, L., Chen, B., Zheng, Y., & Xiao, J. (2017). Hydration properties and binding capacities of dietary fibers from bamboo shoot shell and its hypolipidemic effects in mice. *Food and Chemical Toxicology, 109*, 1003–1009. https://doi.org/10.1016/j.fct.2017.02.029

Ma, M., & Mu, T. (2016). Effects of extraction methods and particle size distribution on the structural, physicochemical, and functional properties of dietary fiber from deoiled cumin. *Food Chemistry, 194*, 237–246. https://doi.org/10.1016/j.foodchem.2015.07.095

Mateos-Aparicio, I. (2021). Chapter 19 - Plant-Based by-products. In C. M. Galanakis (Ed.), *Food waste recovery* (2nd ed., pp. 367–397). Academic Press. https://doi.org/10.1016/B978-0-12-820563-1.00022-6.

Meng, X. H., Wu, C. C., Liu, H. Z., Tang, Q. W., & Nie, X. H. (2021). Dietary fibers fractionated from gardenia (*Gardenia jasminoides* ellis) husk: Structure and *In Vitro* hypoglycemic effect. *Journal of the Science of Food and Agriculture, 101*(9), 3723–3731. https://doi.org/10.1002/jsfa.11003

Moczkowska, M., Karp, S., Niu, Y. G., & Kurek, M. A. (2019). Enzymatic, enzymatic-ultrasonic and alkaline extraction of soluble dietary fibre from flaxseed - A physicochemical approach. *Food Hydrocolloids, 90*, 105–112. https://doi.org/10.1016/j.foodhyd.2018.12.018

Murray, B. S., Durga, K., Yusoff, A., & Stoyanov, S. D. (2011). Stabilization of foams and emulsions by mixtures of surface active food-grade particles and proteins. *Food Hydrocolloids, 25*(4), 627–638.

Nasrollahzadeh, M., Nezafat, Z., Shafiei, N., & Soleimani, F. (2021). *Polysaccharides in food industry. biopolymer-based metal nanoparticle chemistry for sustainable applications. Iran.* Elsevier.

Qiu, S., Yadav, M. P., & Yin, L. (2017). Characterization and functionalities study of hemicellulose and cellulose components isolated from sorghum bran, bagasse and biomass. *Food Chemistry, 230*, 225–233. https://doi.org/10.1016/j.foodchem.2017.03.028

Sánchez-Zapata, E., Fuentes-Zaragoza, E., Fernández-López, J., Sendra, E., Sayas, E., Navarro, C., & Pérez-Alvarez, J. A. (2009). Preparation of dietary fiber powder from tiger nut (*Cyperus esculentus*) milk ("Horchata") byproducts and its physicochemical properties. *Journal of Agricultural and Food Chemistry, 57*(17), 7719–7725. https://doi.org/10.1021/jf901687r

Selvamuthukumaran, M., & Shi, J. (2017). Recent advances in extraction of antioxidants from plant by-products processing industries. *Food Quality and Safety, 1*(1), 61–81.

Vârban, R., Crișan, I., Vârban, D., Ona, A., Olar, L., Stoie, A., & Ștefan, R. (2021). Comparative FT-IR prospecting for cellulose in stems of some fiber plants: Flax, velvet leaf, hemp and jute. *Applied Sciences, 11*(18), 8570.

Wang, L., Fan, R., Yan, Y. H., Yang, S., Wang, X. S., & Zheng, B. Q. (2023). Characterization of the structural, physicochemical, and functional properties of soluble dietary fibers obtained from the peanut shell using different extraction methods. *Frontiers in Nutrition, 9*, Article 1103673. https://doi.org/10.3389/fnut.2022.1103673

Wang, C. H., Ma, Y. L., Zhu, D. Y., Wang, H., Ren, Y. F., Zhang, J. G., Thakur, K., & Wei, Z. J. (2017). Physicochemical and functional properties of dietary fiber from bamboo shoots (*Phyllostachys praecox*). *Emirates Journal of Food and Agriculture, 29*(7), 509–517. https://doi.org/10.9755/ejfa.2017-02-274

Wen, Y., Niu, M., Zhang, B., Zhao, S., & Xiong, S. (2017). Structural characteristics and functional properties of rice bran dietary fiber modified by enzymatic and enzyme-micronization treatments. *LWT, 75*, 344–351. https://doi.org/10.1016/j.lwt.2016.09.012

Wong, K. H., & Cheung, P. C. K. (2005). Dietary fibers from mushroom sclerotia: 1. Preparation and physicochemical and functional properties. *Journal of Agricultural and Food Chemistry, 53*(24), 9395–9400. https://doi.org/10.1021/jf0510788

Wu, Q. L., Zhang, M., Hu, H. P., Tu, Y., Gao, P. H., Li, T., Zhang, X. X., Teng, J., & Wang, L. (2024). Comparative study on chemical composition, functional properties of dietary fibers prepared from four China cereal brans. *International Journal of Biological Macromolecules, 257*, Article 128510. https://doi.org/10.1016/j.ijbiomac.2023.128510

Xie, F., Li, M., Lan, X., Zhang, W., Gong, S., Wu, J., & Wang, Z. (2017). Modification of dietary fibers from purple-fleshed potatoes (heimeiren) with high hydrostatic pressure and high pressure homogenization processing: A comparative study. *Innovative Food Science & Emerging Technologies, 42*, 157–164.

Yamazaki, E., Murakami, K., & Kurita, O. (2005). Easy preparation of dietary fiber with the high water-holding capacity from food sources. *Plant Foods for Human Nutrition, 60*(1), 17–23. https://doi.org/10.1007/s11130-005-2537-9

Yan, L., Li, T., Liu, C., & Zheng, L. (2019). Effects of high hydrostatic pressure and superfine grinding treatment on physicochemical/functional properties of pear pomace and chemical composition of its soluble dietary fibre. *LWT, 107*, 171–177. https://doi.org/10.1016/j.lwt.2019.03.019

Zambrano, M., Meléndez, R., & Gallardo, Y. (2001). Propiedades funcionales y metodología para su evaluación en fibra dietética. In M. F. Editado por Lajolo, F. Saura-Calixto, E. Witting, & E. y Wenzel (Eds.), *Fibra Dietética en Iberoamérica: Tecnología y Salud. Obtención, caracterización, efecto fisiológico y aplicación en alimentos* (pp. 195–209). Varela Editora Brasil.

Zhang, S., Ma, Q., Deng, M., Jia, X., Huang, F., Dong, L., Zhang, R., Sun, Z., & Zhang, M. (2024). Composition, structural, physicochemical and functional properties of dietary fiber from different milling fractions of Black rice bran. *Lwt-Food Science and Technology, 195*, Article 115743. https://doi.org/10.1016/j.lwt.2024.115743

Zhang, S., Xu, X., Cao, X., & Liu, T. (2023). The structural characteristics of dietary fibers from Tremella fuciformis and their hypolipidemic effects in mice. *Food Science and Human Wellness, 12*(2), 503–511. https://doi.org/10.1016/j.fshw.2022.07.052

Zhang, W., Zeng, G., Pan, Y., Chen, W., Huang, W., Chen, H., & Li, Y. (2017). Properties of soluble dietary fiber-polysaccharide from papaya peel obtained through alkaline or ultrasound-assisted alkaline extraction. *Carbohydrate Polymers, 172*, 102–112.

Zhu, Y., Chu, J. X., Lu, Z. X., Lv, F. X., Bie, X. M., Zhang, C., & Zhao, H. Z. (2018). Physicochemical and functional properties of dietary fiber from foxtail millet (*setaria Italic*) bran. *Journal of Cereal Science, 79*, 456–461. https://doi.org/10.1016/j.jcs.2017.12.011

Zou, X. Q., Xu, X. L., Chao, Z. H., Jiang, X., Zheng, L., & Jiang, B. Z. (2022). Properties of plant-derived soluble dietary fibers for fiber-enriched foods: A comparative evaluation. *International Journal of Biological Macromolecules, 223*, 1196–1207. https://doi.org/10.1016/j.ijbiomac.2022.11.008